

# Ab Initio Classical Trajectory Study of the Dissociation of Neutral and Positively Charged Methanimine ( $\text{CH}_2\text{NH}^{n+}$ $n = 0-2$ )

Jia Zhou and H. Bernhard Schlegel\*

Department of Chemistry, Wayne State University, Detroit, Michigan 48202

Received: June 9, 2009; Revised Manuscript Received: July 24, 2009

The structures and energetics of the reactants, intermediates, transition states, and products for the dissociation of methanimine neutral, monocation, dication, and trication were calculated at the CBS-APNO level of theory. The dissociations of the neutral, monocation, and dication were studied by ab initio direct classical trajectory calculations at the B3LYP/6-311G(d,p) level of theory. A microcanonical ensemble using quasiclassical normal mode sampling was constructed by distributing 200, 150, and 120 kcal/mol of excess energy above the local minima of the neutral, singly, and doubly charged species, respectively. Many of the trajectories dissociate directly to produce  $\text{H}^+$ , H atom, or  $\text{H}_2$ . However, for a fraction of the cases, substantial migration of the hydrogen occurs within the molecule before dissociation. The preferred dissociation product for the neutral and the monocation is hydrogen atom. Elimination of  $\text{H}_2$  was seen in 20% of the trajectories for the neutral and in 5% of the trajectories for the monocation. Dissociations of the dication and trication produced  $\text{H}^+$  rather than H atom.  $\text{HCNH}^+$  was formed in 85–90% of the dissociating trajectories for the monocation and dication.

## Introduction

The simplest example of a molecule with a carbon–nitrogen double bond is  $\text{H}_2\text{C}=\text{NH}$ , known variously as methanimine, methyleneimine, and formaldimine. Similar to ethylene and formaldehyde, the simplest examples of CC and CO double bonds, the low-energy dissociation channels of  $\text{H}_2\text{CNH}$  are loss of hydrogen atom and elimination of molecular  $\text{H}_2$ . Ionization to form the monocation simplifies the potential energy surface and reduces the barriers to rearrangement and dissociation. Formation of the dication favors dissociation into two monocations and should reduce the barriers further. When a third electron is removed, the barriers are less than 5 kcal/mol (see below) and the molecule dissociates via a Coulomb explosion. In the present paper, we use accurate computational methods to explore the potential energy surfaces of  $\text{H}_2\text{CNH}$  and its cations and use ab initio classical trajectory calculations to examine the molecular dynamics of these systems.

Neutral  $\text{H}_2\text{CNH}$  is a reactive intermediate that can be produced by pyrolysis of amines and azides.<sup>1–5</sup> It has also been observed in interstellar dust clouds.<sup>6</sup> The gas-phase structure has been determined by microwave spectroscopy.<sup>1</sup> The infrared spectrum has been observed in early matrix isolation experiments<sup>7,8</sup> and later in the gas phase.<sup>3,9–12</sup> The electronic spectrum of  $\text{H}_2\text{CNH}$  has been reported only recently.<sup>13</sup> The best values for heat of formation of  $\text{H}_2\text{CNH}$  obtained experimentally ( $22 \pm 3$  kcal/mol<sup>14</sup>) and computationally ( $21.1 \pm 0.5$  kcal/mol<sup>15</sup>) are in good agreement. In the numerous computational studies,<sup>16–25</sup> the aminocarbene isomer,  $\text{HCNH}_2$ , is found to be 35–39 kcal/mol higher than  $\text{H}_2\text{CNH}$ , and singlet methylnitrene,  $\text{CH}_3\text{N}$ , is calculated to be ca. 89 kcal/mol above  $\text{H}_2\text{CNH}$ . Aminocarbene can be produced by pyrolysis of aminocyclopropane.<sup>26</sup> Singlet methylnitrene can be generated by pyrolysis of methyl azide,  $\text{CH}_3\text{N}_3$ ,<sup>27</sup> but calculations show that there is little or no barrier for singlet  $\text{CH}_3\text{N}$  to rearrange to  $\text{H}_2\text{CNH}$ .<sup>16–19,21–25</sup> Dissociation of  $\text{H}_2\text{CNH}$  has been studied

experimentally and computationally.<sup>17–20,24,27</sup> It can occur by loss of hydrogen atom from either the carbon or the nitrogen with barriers of 85–95 kcal/mol to form  $\text{HCNH}$  and  $\text{H}_2\text{CN}$ , which can lose another hydrogen atom with barriers of 30–35 kcal/mol to produce  $\text{HCN}$ .<sup>18,28–30</sup> Alternatively,  $\text{H}_2\text{CNH}$ ,  $\text{HCNH}_2$ , and  $\text{CH}_3\text{N}$  can dissociate by 1,1- or 1,2- $\text{H}_2$  eliminations with barriers of 85–100 kcal/mol above  $\text{H}_2\text{CNH}$ .<sup>18–20,24</sup>

Various isomers of  $\text{H}_2\text{CNH}$  monocation can be generated from the decomposition of methylamine, cyclopropylamine, azetidine, and aminocarbenium ion and by the reaction of  $\text{C}^+$  with  $\text{NH}_3$ .<sup>20,26,31–33</sup> Ab initio calculations show that the  $\text{HCNH}_2^+$  isomer is ca. 4 kcal/mol more stable than  $\text{H}_2\text{CNH}^+$  and is separated from the latter by a barrier of ca. 57 kcal/mol.<sup>17,34–36</sup> The lowest energy dissociation channels involve loss of hydrogen atom.<sup>34,35</sup> Of the three possible singlet products resulting from H dissociation,  $\text{HCNH}^+$  is the most stable,  $\text{CNH}_2^+$  is a minimum lying ca. 52 kcal/mol higher, and  $\text{H}_2\text{CN}^+$  is a saddle point ca. 74 kcal/mol above  $\text{HCNH}^+$ .<sup>37–41</sup> Loss of  $\text{H}_2$  from  $\text{H}_2\text{CNH}^+/\text{HCNH}_2^+$  leads to  $\text{HNC}^+$  and  $\text{HCN}^+$  with the former being 23 kcal/mol more stable than the latter.<sup>42–46</sup>

By comparison to neutral  $\text{H}_2\text{CNH}$  and the monocation, very few papers have examined the potential energy surface of the dication.<sup>47,48</sup> The most stable singlet dication isomer is  $\text{HCNH}_2^{2+}$ .  $\text{CNH}_3^{2+}$  is 48 kcal/mol higher and has a barrier of ca. 30 kcal/mol for conversion to  $\text{HCNH}_2^{2+}$ .  $\text{H}_2\text{CNH}^{2+}$  is either a saddle point or a very shallow minimum ca. 45 kcal/mol above  $\text{HCNH}_2^{2+}$ .  $\text{H}_3\text{CN}^{2+}$  dissociates to  $\text{HCN}^{2+} + \text{H}_2$ . Barriers of 40–65 kcal/mol separate  $\text{HCNH}_2^{2+}$  and  $\text{CNH}_3^{2+}$  from dissociation products  $\text{H}^+$  plus  $\text{HCNH}^+$  and  $\text{CNH}_2^+$ . No studies appear to have been published on the potential energy surface of the trication.

The potential energy surfaces for the dissociation of  $\text{H}_2\text{CNH}$  and its positively charged ions that have been published over the past three decades involve a wide variety of computational methods. The differing accuracies of these methods make comparisons somewhat difficult. In the present paper, we use high-level ab initio calculations to provide a consistent and

\* To whom correspondence should be addressed.

accurate description of the structures and energetics of neutral  $\text{H}_2\text{CNH}$  and its cations on the ground-state potential energy surfaces, and we employ Born–Oppenheimer classical trajectory calculations at the B3LYP/6-311G(d,p) level to examine the dynamics of the dissociation of these species.

## Method

The Gaussian suite of programs<sup>49</sup> was used for the ab initio electronic structure and molecular dynamics calculations. The geometries of the minima and the transition states were optimized by hybrid density functional theory (B3LYP<sup>50–52</sup>), second-order Møller–Plesset perturbation theory (MP2<sup>53</sup>), and quadratic configuration interaction (QCISD<sup>54</sup>) methods. The spin restricted vs unrestricted stability of each structure was tested using standard methods<sup>55</sup> (see Table S1 of the Supporting Information). The CBS-APNO complete basis set extrapolation method of Montgomery et al.<sup>56</sup> was used to compute accurate energy differences. The CBS-APNO calculations have a mean absolute deviation of 0.5 kcal/mol for heats of reaction. Because singlet  $\text{CH}_3\text{N}$  requires a multireference treatment, its energy was estimated by adding the singlet–triplet energy difference calculated at the CASPT2/cc-pVTZ level of theory<sup>25</sup> to the triplet energy calculated by CBS-APNO.

Ab initio classical trajectories were computed at the B3LYP/6-311G(d,p) level of theory using a Hessian-based predictor–corrector method.<sup>57,58</sup> A predictor step is taken on the quadratic surface obtained from the energy, gradient, and Hessian from the beginning point. A fifth-order polynomial is then fitted to the energies, gradients, and Hessians at the beginning and end points of the predictor step, and the Bulirsch–Stoer algorithm<sup>59</sup> is used to take a corrector step on this fitted surface with the angular forces projected out. The Hessians are updated for five steps before being recalculated analytically. The trajectories were terminated when the centers of mass of the fragments were 10 bohr apart and the gradient between the fragments was less than  $1 \times 10^{-5}$  hartree/bohr. A step size of 0.25 amu<sup>1/2</sup> bohr was used for integrating the trajectories. Each electronic structure calculation was started with an unrestricted initial guess (using the GUESS=MIX keyword in Gaussian) to permit homolytic bond dissociation. The energy was conserved to better than  $1 \times 10^{-5}$  hartree, and the angular momentum was conserved to  $1 \times 10^{-8} \hbar$ .

Trajectories were initiated at the local minima,  $\text{H}_2\text{CNH}$ ,  $\text{H}_2\text{CNH}^+$ , and  $\text{H}_2\text{NCH}^{2+}$  (the dication  $\text{H}_2\text{CNH}^{2+}$  is a first-order saddle point while  $\text{H}_2\text{NCH}^{2+}$  is a local minimum). A microcanonical ensemble of initial states was constructed using the quasi-classical normal mode sampling.<sup>60,61</sup> A total energy of 200, 150, and 120 kcal/mol above the zero point energy of  $\text{H}_2\text{CNH}$ ,  $\text{H}_2\text{CNH}^+$ , and  $\text{H}_2\text{NCH}^{2+}$  was distributed among the nine vibrational modes. The total angular momentum was set to zero corresponding to a rotationally cold distribution, and the phases of the vibrational modes were chosen randomly. For each initial condition, the momentum and displacement were scaled so that the desired total energy was the sum of the vibrational kinetic energy and the potential energy obtained from the ab initio surface. A total of about 200 trajectories for each case were integrated for up to 400 fs starting from the local minima and ending when the products were well-separated.

## Results and Discussion

**Structures and Energetics.** The structures, selected geometrical parameters, and CBS-APNO relative energies of reactants, intermediates, transition states, and products for the dissociation of  $\text{H}_2\text{CNH}^{m+}$  are collected in Figures 1–4 and S1–S4 in the Supporting Information. The neutral, monocation,

dication, and trication structure numbers have prefixes of N, C, D, and T, respectively; the numbering of the structures is according to the potential energy profiles in Figures 1–4 (top to bottom in each column, left column to right column). Relative energies at the B3LYP/6-311G(d,p), MP2/6-311G(d,p), and CBS-APNO levels of theory are compared in Table 1. Generally, B3LYP gives better agreement with the CBS-APNO energies than MP2 (mean absolute deviation of 3.0 and 4.7 kcal/mol, respectively). Adiabatic ionization energies are compared in Table 2. The CBS-APNO values for  $\text{H}_2\text{CNH}$  and HCN are within 0.05 eV of the experimental values (9.97 and 13.60 eV, respectively).

**Neutral  $\text{H}_2\text{CNH}$ .** The key equilibrium structures and transition states on the potential energy surface for  $\text{H}_2\text{CNH}$  isomerization and dissociation are collected in Figure S1 of the Supporting Information. The relative energies of these structures at the CBS-APNO level of theory are plotted in Figure 1.  $\text{HCNH}_2$  (structure N-7) lies ca. 35 kcal/mol higher in energy than  $\text{H}_2\text{CNH}$  (N-1), which is in good accord with previous results.<sup>16–25</sup> Isomerization from  $\text{H}_2\text{CNH}$  to  $\text{HCNH}_2$  occurs more readily via N-TS3 with the H migrating in the plane of *cis*- $\text{HCNH}$  than via N-TS2 with the H migrating across the  $\pi$  bond of *trans*- $\text{HCNH}$ . Dissociation of  $\text{HCNH}_2$  to  $\text{HCN} + \text{H}_2$  (N-17) can occur by a transition state with  $\text{H}_2$  cis or trans to the CH bond (N-TS9 and N-TS8, respectively). The  $\text{HCN} + \text{H}_2$  products can also be reached from  $\text{H}_2\text{CNH}$  via singlet  $\text{CH}_3\text{N}$  (N-4). There is little or no barrier for  $^1\text{A}'$   $\text{CH}_3\text{N}$  isomerizing back to  $\text{CH}_2\text{NH}$ .<sup>16–19,21–25</sup> The transition state for  $\text{CH}_3\text{N} \rightarrow \text{HCN} + \text{H}_2$  (N-TS10) is ca. 10 kcal/mol lower than for  $\text{HCNH}_2 \rightarrow \text{HCN} + \text{H}_2$ . The lowest energy molecular dissociation pathway for  $\text{H}_2\text{CNH}$  leads to the higher energy  $\text{HNC} + \text{H}_2$  product (N-16) and can occur with the  $\text{H}_2$  either cis or trans to the NH bond (N-TS-6 and N-TS5, respectively).

Aside from the thermodynamically favorable  $\text{H}_2$  molecule elimination channels, there are also several H atom dissociation channels to consider. Hydrogen atom dissociations from  $\text{H}_2\text{CNH}$  and  $\text{HCNH}_2$  to form  $\text{H}_2\text{CN}$  (N-15), *cis*- $\text{HCNH}$  (N-12), *trans*- $\text{HCNH}$  (N-13), and  $\text{H}_2\text{NC}$  (N-11) radicals are expected to occur without a reverse barrier. If the hydrogen atom does not depart promptly, it can abstract another hydrogen to form  $\text{H}_2$  plus HCN or HNC. This process has been well documented in formaldehyde and acetaldehyde dissociation and has been termed the “roaming atom” mechanism.<sup>62–68</sup> Isomerization and dissociations of  $\text{H}_2\text{CN}$ ,  $\text{HCNH}$ , and  $\text{H}_2\text{NC}$  have been studied previously.<sup>18,28–30</sup> Dissociations of H atom from these species to form HCN or HNC involve barriers of 22–34 kcal/mol at the CBS-APNO level of theory and occur via transition states N-TS18–N-TS21. A final hydrogen atom dissociation from HCN and HNC leads to CN radical. Alternatively, a free H atom could abstract a hydrogen to yield  $\text{H}_2 + \text{CN}$ . The latter has been studied comprehensively in previous theoretical work.<sup>69,70</sup>

**Monocation.** Figures 2 and S2 summarize the energetics and structures for  $\text{H}_2\text{CNH}^{m+}$  radical cation.  $\text{H}_2\text{CNH}^{+}$  (C-1) lies 4 kcal/mol higher in energy than the  $\text{HCNH}_2^{+}$  isomer (C-6), which is in good accord with the previous results.<sup>35</sup> Like the neutral case, the barrier for isomerization from  $\text{H}_2\text{CNH}^{+}$  to  $\text{HCNH}_2^{+}$  is lower for the proton migrating in the plane of *cis*- $\text{HCNH}$  (C-TS4, 42 kcal/mol) than across the  $\pi$  bond in *trans*- $\text{HCNH}$  (C-TS3, 55 kcal/mol). Barriers for loss of hydrogen atom from  $\text{HCNH}_2^{+}$  and  $\text{H}_2\text{CNH}^{+}$  to form  $\text{HCNH}^+ + \text{H}$  (C-10) are 43 and 31 kcal/mol via C-TS8 and C-TS5, respectively.  $\text{HCNH}_2^{+}$  can also dissociate to produce  $\text{CNH}_2^+ + \text{H}$ , C-7, but this requires 82 kcal/mol. Isomerization of  $\text{CNH}_2^+$  to  $\text{HCNH}^+$  has a barrier of 19 kcal/mol (C-TS9).  $\text{H}_2\text{CN}^+$  (C-TS2) is a

**TABLE 1: Relative Energies (in kcal/mol) of the Various Points on the H<sub>2</sub>CNH, H<sub>2</sub>CNH<sup>+</sup>, HCNH<sub>2</sub><sup>2+</sup>, and HCNH<sub>2</sub><sup>3+</sup> Potential Energy Surfaces**

	B3LYP 6-311G(d,p)	MP2 6-311G(d,p)	CBS-APNO
<b>Neutral</b>			
N-1	0.0	0.0	0.0
N-TS2	88.9	91.6	88.9
N-TS3	80.5	83.2	81.8
N-4 <sup>a</sup>	80.7	86.1	86.0
N-TS5	84.0	90.0	85.8
N-TS6	83.6	90.8	84.6
N-7	34.6	38.4	35.6
N-TS8	103.0	118.2	106.7
N-TS9	97.8	107.6	100.5
N-TS10	92.9	108.9	95.7
N-11	113.1	113.6	117.6
N-12	95.6	98.7	99.1
N-13	91.5	93.7	94.4
N-TS14	129.5	129.7	131.1
N-15	82.8	90.1	86.7
N-16	22.7	19.5	22.5
N-17	8.4	0.8	8.2
N-TS18	135.6	138.7	140.3
N-TS19	126.7	120.9	128.7
N-TS20	117.3	120.9	121.2
N-TS21	115.8	119.4	117.5
N-22	126.4	113.8	126.3
N-23	112.0	95.1	111.9
N-TS24	135.4	145.3	136.6
N-25	134.8	141.5	133.2
MAD	2.1	5.1	
<b>Monocation</b>			
C-1	0.0	0.0	0.0
C-TS2	100.2	94.4	98.7
C-TS3	55.7	52.4	54.7
C-TS4	47.2	41.2	42.2
C-T5	34.2	29.1	31.2
C-6	-2.8	-9.2	-3.8
C-7	83.1	69.3	78.7
C-TS8	39.9	39.7	39.0
C-TS9	103.8	87.1	97.8
C-10	33.5	12.1	26.9
C-11	94.4	90.5	93.6
C-12	77.6	70.7	70.9
MAD	3.1	4.5	
<b>Dication</b>			
D-1	0.0	0.0	0.0
D-TS2	76.9	78.5	73.1
D-TS3	63.6	66.6	64.5
D-4	53.7	54.7	50.6
D-TS5	41.5	39.4	41.5
D-6	-5.7	-4.5	-7.9
D-TS7	111.0	118.6	99.2
D-TS8	15.0	13.2	11.2
D-9	6.0	1.2	2.0
D-10	-55.3	-61.7	-59.7
MAD	3.4	4.1	
<b>Trication</b>			
T-1	0.0	0.0	0.0
T-TS2	3.2	4.3	3.5
T-TS3	0.7	0.9	1.9
T-4	-225.2	-225.0	-231.2
T-TS5	-193.0	-194.8	-199.3
T-TS6	-198.1	-199.7	-205.3
T-7	-239.1	-238.8	-244.4
T-8	-297.3	-300.2	-307.9
T-TS9	-200.2	-198.9	-203.5
T-10	-280.4	-280.4	-285.2
MAD	4.5	4.1	
MAD overall	3.0	4.7	

<sup>a</sup> Because singlet CH<sub>3</sub>N requires a multireference treatment, its energy was estimated by adding the singlet-triplet energy difference calculated at the CASPT2/cc-pVTZ level of theory<sup>25</sup> to the energy calculated for the triplet.

saddle point and 72 kcal/mol above HCNH<sup>+</sup>. Dissociation of molecular hydrogen from HCNH<sub>2</sub><sup>2+</sup> and H<sub>2</sub>CNH<sup>+</sup> could occur by 1,1-H<sub>2</sub> or 1,2-H<sub>2</sub> elimination to produce HNC<sup>+</sup> + H<sub>2</sub> (C-12) or HCN<sup>+</sup> + H<sub>2</sub> (C-11). Since these H<sub>2</sub> eliminations are rather endothermic (e.g., 75 and 97 kcal/mol from HCNH<sub>2</sub><sup>2+</sup>), H atom loss is the preferred channel for the dissociation of

**TABLE 2: Adiabatic Ionization Potentials (eV)**

	B3LYP 6-311G(d,p)	MP2 6-311G(d,p)	CBS-APNO
H <sub>2</sub> CNH	9.73	9.90	9.94
HCNH <sub>2</sub>	8.11	7.84	8.23
HCNH <sub>2</sub> <sup>+</sup>	17.64	17.20	17.52
HCNH <sub>2</sub> <sup>2+</sup>	30.56	30.57	30.78
HCNH	7.21	6.36	7.01
HCNH <sup>+</sup>	22.59	22.90	22.76
CNH <sub>2</sub>	8.43	7.98	8.25
CNH <sub>2</sub> <sup>+</sup>	21.04	21.01	21.09
HCN	13.46	13.79	13.64
HNC	12.11	12.12	12.04

HCNH<sub>2</sub><sup>2+</sup> and H<sub>2</sub>CNH<sup>+</sup>. Hydrogen abstraction by a roaming atom mechanism<sup>62–68</sup> is also unlikely because these reactions are quite endothermic (44 and 67 kcal/mol for HCNH<sup>+</sup> + H → HNC<sup>+</sup> + H<sub>2</sub> and HCN<sup>+</sup> + H<sub>2</sub>, respectively). The HNC<sup>+</sup> is found to be 23 kcal/mol more stable than HCN<sup>+</sup>, which is in agreement with earlier work.<sup>42–46</sup>

**Dication.** The energetics and structures for the singlet dication potential energy surface are collected in Figures 3 and S3. Similar to the monocation, HCNH<sub>2</sub><sup>2+</sup> (D-1) is the most stable structure. Even though the dication is isoelectronic with protonated acetylene, C<sub>2</sub>H<sub>3</sub><sup>+</sup>, there is no indication of a stable bridged structure.<sup>71–79</sup> In previous calculations, H<sub>2</sub>CNH<sub>2</sub><sup>2+</sup> was found to be a higher lying minimum at the HF and MP2 levels of theory.<sup>47,48</sup> We also find it to be a minimum at MP2 but with a barrier of less than 5 kcal/mol for conversion to H<sub>2</sub>CNH<sub>2</sub><sup>2+</sup>. More highly correlated methods (CCSD, CCSD(T), and BD with 6-311+G(d,p) and 6-311+G(3df,2pd) basis sets) show that H<sub>2</sub>CNH<sub>2</sub><sup>2+</sup> is a saddle point (see Figure S5 and Table S2 in the Supporting Information). The small magnitude of the imaginary frequency (170*i*–273*i*) indicates that the potential energy surface is rather flat. A few density functionals (BMK, M052X, mPW1PW91, and PBE1PBE) find H<sub>2</sub>CNH<sub>2</sub><sup>2+</sup> to be a saddle point, while other functionals (BLYP, PBE, PW91, and TPSS) find it to be a shallow local minimum (Table S2 in the Supporting Information). For B3LYP and TPSSh, H<sub>2</sub>CNH<sub>2</sub><sup>2+</sup> is a saddle point with the 6-311+G(3df,2pd) basis set, but it is a shallow minimum with the 6-311+G(d,p) basis set. In agreement with earlier calculations, CNH<sub>3</sub><sup>2+</sup> (D-4) is a stable minimum 51 kcal/mol above HCNH<sub>2</sub><sup>2+</sup> and is separated from it by a barrier of 22 kcal/mol.

The lowest energy channel for dissociation of HCNH<sub>2</sub><sup>2+</sup> is loss of a proton to give HCNH<sup>+</sup> (D-10, -60 kcal/mol) with a barrier of 41 kcal/mol (D-TS5). Loss of a proton from HCNH<sub>2</sub><sup>2+</sup> to form CNH<sub>2</sub><sup>+</sup> (D-6) is less exothermic (-8 kcal/mol) and has a higher barrier (D-TS3, 65 kcal/mol). For the deprotonation of dications, AH<sup>2+</sup> → A<sup>+</sup> + H<sup>+</sup>, careful attention must be paid to spin restricted vs unrestricted instabilities.<sup>80</sup> If the second ionization potential of A (A<sup>+</sup> → A<sup>2+</sup> + e<sup>-</sup>) is comparable to the ionization potential of hydrogen (13.6 eV), then spin-unrestricted methods must be used. Since the ionization potentials of HCNH<sup>+</sup> and CNH<sub>2</sub><sup>+</sup> are 21–23 eV (see Table 2), spin-restricted calculations are satisfactory for the deprotonation of HCNH<sub>2</sub><sup>2+</sup> as confirmed by stability calculations on transition-states D-TS3 and D-TS5 (see Table S1 in the Supporting Information).

**Trication.** Figures 4 and S4 summarize the energetics and structures for the trication. Surprisingly, HCNH<sub>2</sub><sup>3+</sup> (T-1) is a local minimum. Dissociation to HCNH<sub>2</sub><sup>2+</sup> + H<sup>+</sup> (T-7) is very exothermic (-244 kcal/mol) and has a barrier of only 2 kcal/mol (T-TS3). Dissociation to CNH<sub>2</sub><sup>2+</sup> + H<sup>+</sup> (T-4) is a little less exothermic (-231 kcal/mol) and has a slightly higher barrier

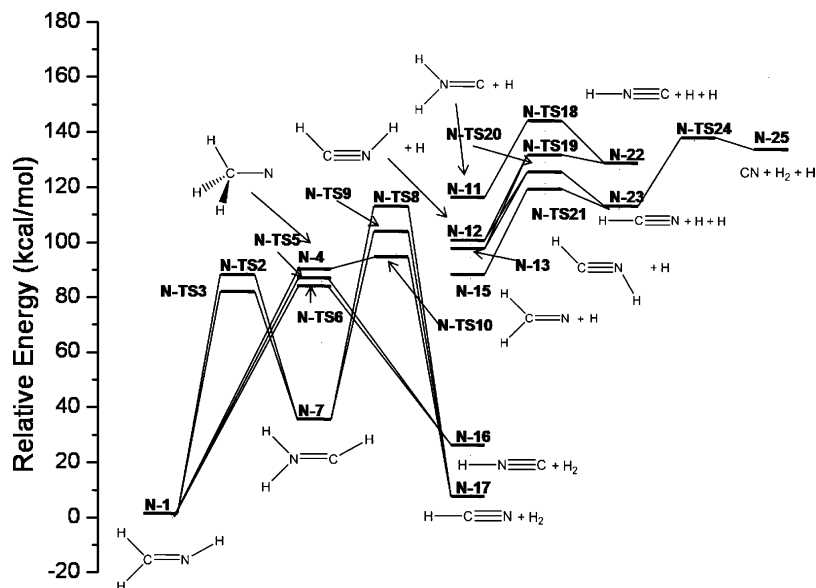


Figure 1. Potential energy profile for the isomerization and dissociation of neutral  $\text{H}_2\text{CNH}$  computed at the CBS-APNO level of theory.

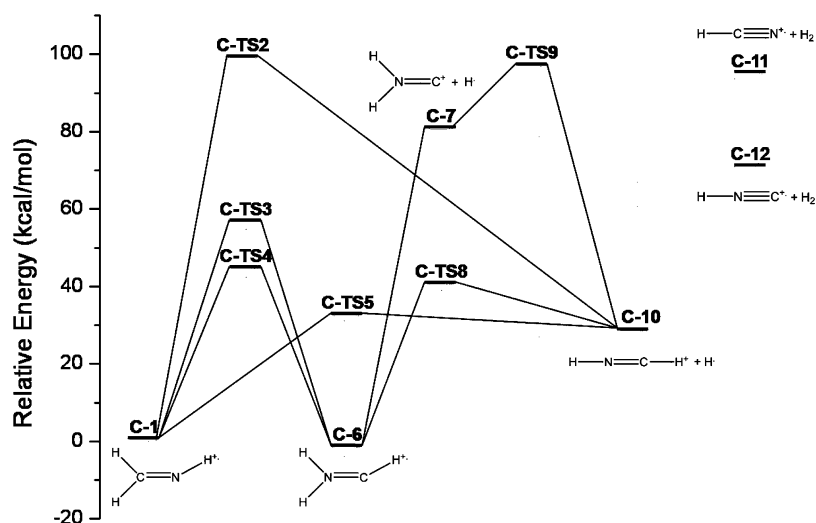


Figure 2. Potential energy profile for the isomerization and dissociation of  $\text{H}_2\text{CNH}^+$  computed at the CBS-APNO level of theory.

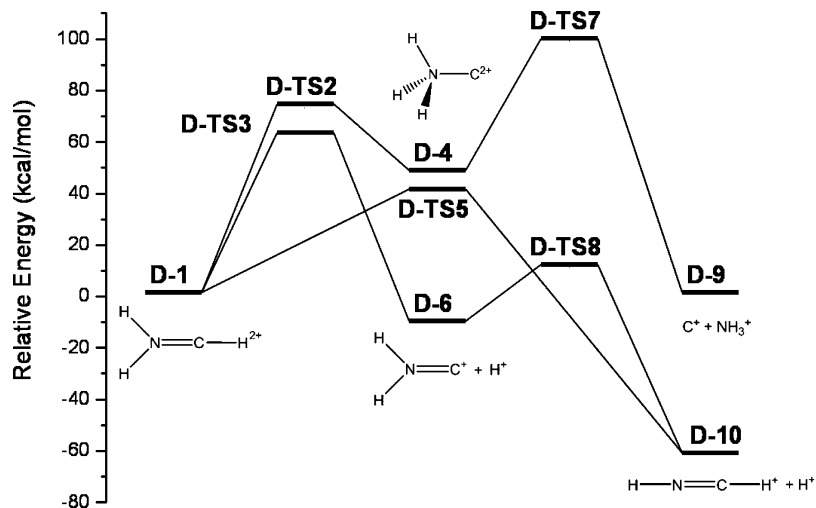
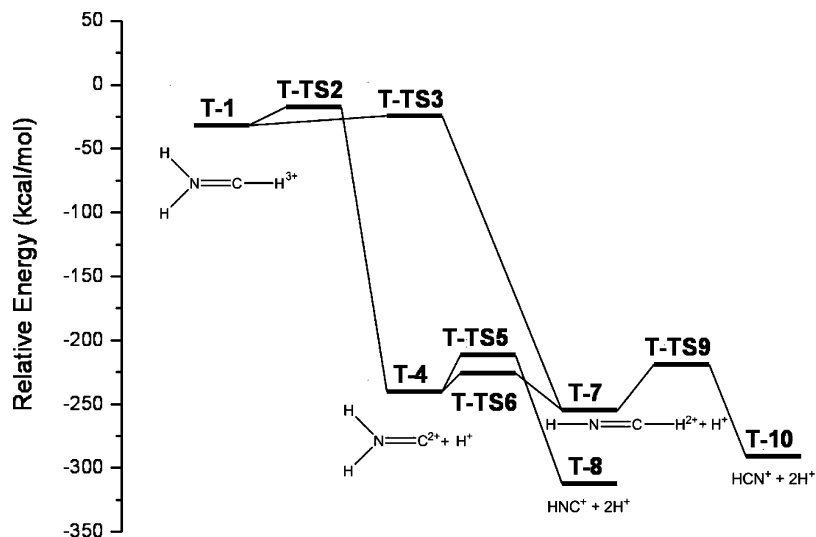


Figure 3. Potential energy profile for the isomerization and dissociation of  $\text{HCNH}_2^{2+}$  computed at the CBS-APNO level of theory.

(T-TS2, 4 kcal/mol).  $\text{HCNH}_2^{2+}$  and  $\text{CNH}_2^{2+}$  can lose another proton to form  $\text{HNC}^+$  and  $\text{HCN}^+$ .

**Dynamics.** Comparison of the data in Table 1 indicates that the B3LYP/6-311G(d,p) level of theory should be suitable for

simulating the molecular dynamics of neutral and charged  $\text{H}_2\text{CNH}$ . The trajectories were started at local minima, namely,  $\text{H}_2\text{CNH}$  for the neutral,  $\text{H}_2\text{CNH}^+$  for the monocation, and  $\text{HCNH}_2^{2+}$  for the singlet dication. Because of the low barriers



**Figure 4.** Potential energy profile for the isomerization and dissociation of  $\text{HCNH}_2^{3+}$  computed at the CBS-APNO level of theory.

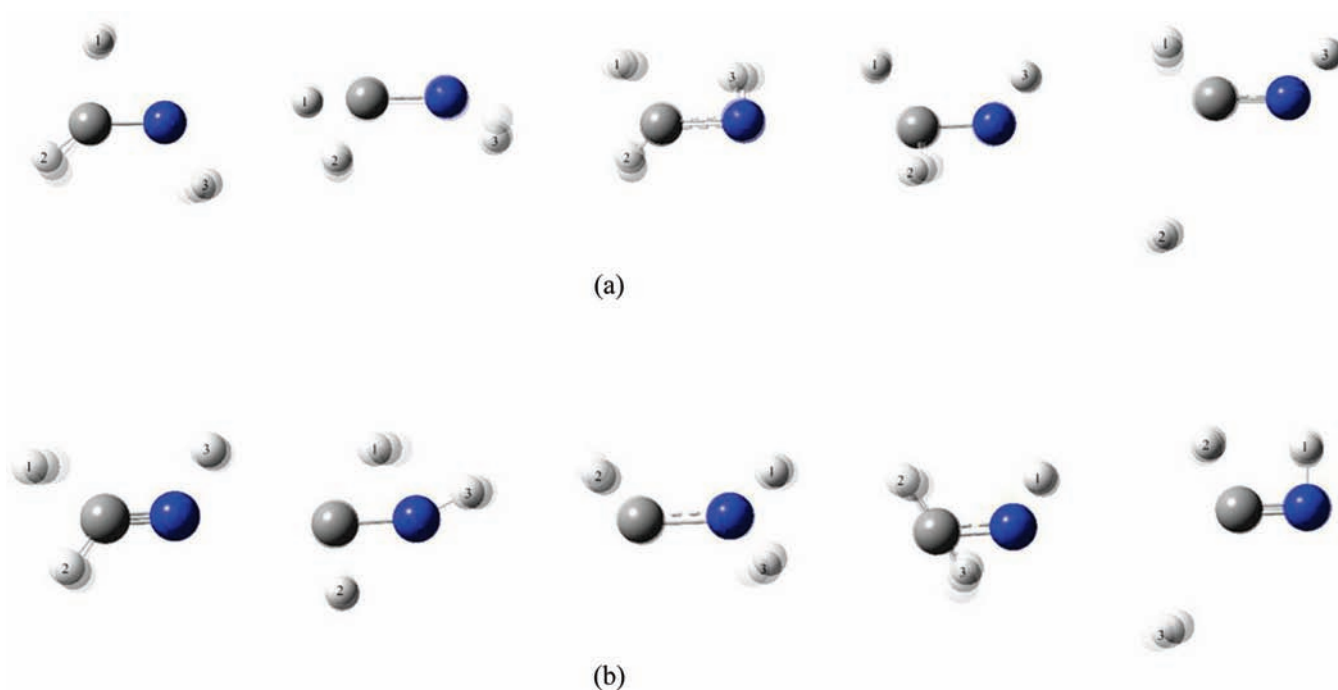


**Figure 5.** Snapshots along typical trajectories for  $\text{H}_2\text{CNH} \rightarrow \text{HCNH} + \text{H}$ : (a) direct dissociation and (b) indirect dissociation. Movies of the trajectories appear in Supporting Information.

for the trication, no trajectories were calculated for  $\text{HCNH}_2^{3+}$ . Approximately 200 trajectories were initiated for each case. The initial energies were chosen so that most trajectories would finish within 400 fs (200, 150, and 120 kcal/mol for the neutral, monocation, and dication, respectively). For these conditions, only dissociations involving  $\text{H}^+$ , H atom, and molecular  $\text{H}_2$  were seen. Trajectories are termed direct if  $\text{H}^+$  or H atom dissociate promptly. For indirect trajectories, hydrogen migrates within the molecule for some time before dissociation occurs. Figure 5 shows two examples of indirect trajectories (the corresponding movies are available in the Supporting Information). Because of the relatively high initial energy,  $\text{H}_2$  dissociation by the roaming mechanism was not observed. The results of the trajectory calculations are summarized in Table 3.

For neutral  $\text{H}_2\text{CNH}$ , 17 trajectories resulted in  $\text{HCN} + \text{H}_2$  (8 by 1,2 elimination; 5 by 1,1 elimination followed by isomerization; 3 by isomerization to  $\text{H}_2\text{CN}$  followed by 1,1 elimination; and 1 by isomerization to  $\text{HCNH}_2$  followed by 1,1 elim-

ination), while 19 produced  $\text{HNC} + \text{H}_2$  (primarily by 1,1 elimination). Even though HCN is more stable, the lower barrier for the direct dissociation of  $\text{H}_2\text{CNH}$  to  $\text{HNC} + \text{H}_2$  leads to more trajectories yielding HNC as a product. Atomic H dissociation is more favorable than molecular  $\text{H}_2$  elimination: 52 trajectories went to  $\text{HCNH} + \text{H}$  directly and 7 indirectly, while 23 went to  $\text{H}_2\text{CN} + \text{H}$  directly and 5 indirectly (because of the large amplitude vibrations, it is not possible to distinguish *cis*- $\text{HCNH}$  and *trans*- $\text{HCNH}$  products in the trajectory calculations). During the simulations, an additional three trajectories lost H atom directly to form  $\text{H}_2\text{CN}$  which then converted to  $\text{HCNH}$ , while one trajectory lost H atom directly to form  $\text{HCNH}$  and then to convert to  $\text{H}_2\text{CN}$ . Because  $\text{CNH}_2$  is much higher in energy, none of the trajectories produced this product. After the dissociation of the first H atom, a second H atom can be lost. Forty trajectories resulted in  $\text{HCN} + \text{H} + \text{H}$ , while 16 yielded  $\text{CNH} + \text{H} + \text{H}$ . The pathway leading to  $\text{CN} + \text{H}_2 +$

**TABLE 3: Branching Ratios for H<sub>2</sub>CNH, H<sub>2</sub>CNH<sup>+</sup>, and HCNH<sub>2</sub><sup>2+</sup> Dissociation Obtained from Molecular Dynamics at the B3LYP/6-311G(d,p) Level of Theory<sup>a</sup>**

product structure	description	branching ratio
<b>Neutral</b>		
HCNH + H	direct dissociation	28.26
HCN + H + H	triple dissociation	21.74
H <sub>2</sub> CN + H	direct dissociation	12.50
CNH + H <sub>2</sub>	molecular elimination	10.33
HCN + H <sub>2</sub>	molecular elimination	9.24
CNH + H + H	triple dissociation	8.70
HCNH + H	indirect dissociation	3.80
H <sub>2</sub> CN + H	indirect dissociation	2.72
HCNH + H	H <sub>2</sub> CN converts to HCNH	1.63
H <sub>2</sub> CN + H	HCNH converts to H <sub>2</sub> CN	0.54
CN + H <sub>2</sub> + H	triple dissociation	0.54
<b>Monocation</b>		
HCNH <sup>+</sup> + H	direct dissociation	67.80
HCNH <sup>+</sup> + H	indirect dissociation	12.68
HCNH <sup>+</sup> + H	H <sub>2</sub> CN <sup>+</sup> converts to HCNH <sup>+</sup>	9.76
H <sub>2</sub> CN <sup>+</sup> + H	direct dissociation	3.41
CNH <sup>+</sup> + H <sub>2</sub>	molecular elimination	2.93
HCN <sup>+</sup> + H <sub>2</sub>	molecular elimination	2.44
CNH <sub>2</sub> <sup>+</sup> + H	direct dissociation	0.98
<b>Dication</b>		
HCNH <sup>+</sup> + H <sup>+</sup>	direct dissociation	51.01
HCNH <sup>+</sup> + H <sup>+</sup>	indirect dissociation	23.89
HCNH <sub>2</sub> <sup>2+</sup>	no dissociation	12.55
CNH <sub>2</sub> <sup>2+</sup> + H <sup>+</sup>	direct dissociation	10.12
HCNH <sup>+</sup> + H <sup>+</sup>	CNH <sub>2</sub> <sup>2+</sup> converts to HCNH <sup>+</sup>	2.02
CNH <sub>2</sub> <sup>2+</sup> + H <sup>+</sup>	indirect dissociation	0.41

<sup>a</sup> Microcanonical ensemble with quasiclassical normal mode sampling with 200, 150, and 120 kcal/mol excess energy above the H<sub>2</sub>CNH, H<sub>2</sub>CNH<sup>+</sup>, and HCNH<sub>2</sub><sup>2+</sup> minima, respectively.

H has the highest barrier of the reactions observed, and only 1 trajectory out of 231 was seen for this channel.

In trajectories of the monocation, HCNH<sup>+</sup> accounts for 90% of the dissociation products. Of the 205 trajectories started from the H<sub>2</sub>CNH<sup>+</sup> minimum, 139 trajectories produce HCNH<sup>+</sup> directly, and 26 produce HCNH<sup>+</sup> indirectly. Another 20 trajectories lost H atom first to produce H<sub>2</sub>CN<sup>+</sup> which then isomerized to the more stable species, HCNH<sup>+</sup>. Seven more trajectories stopped at H<sub>2</sub>CN<sup>+</sup> + H product within the 400 fs simulation time. Since H<sub>2</sub>CN<sup>+</sup> is a transition state, further propagation of these trajectories would yield HCNH<sup>+</sup>. Two additional trajectories produced CNH<sub>2</sub><sup>+</sup> + H, which is separated from HCNH<sup>+</sup> + H by a barrier of ca. 20 kcal/mol. Two H<sub>2</sub> molecule elimination channels were also observed: five trajectories resulted in HCN<sup>+</sup> + H<sub>2</sub> and six trajectories produced CNH<sup>+</sup> + H<sub>2</sub>, each occurring by both 1,1 and 1,2-H<sub>2</sub> elimination.

For the dication, a total of 247 trajectories were integrated starting from HCNH<sub>2</sub><sup>2+</sup> with an initial energy of 120 kcal/mol. The major product is HCNH<sup>+</sup> + H<sup>+</sup> with 126 trajectories resulting in direct dissociation and 59 trajectories resulting in indirect. Only a few trajectories produced CNH<sub>2</sub><sup>2+</sup> + H<sup>+</sup>: 25 direct and 1 indirect. Additionally, five trajectories first formed CNH<sub>2</sub><sup>2+</sup> + H<sup>+</sup> and then converted to the more stable species, HCNH<sup>+</sup>. There were also 31 trajectories that did not dissociate completely in the 400 fs simulation time.

## Summary

The energetics of neutral and positively charged H<sub>2</sub>CNH dissociations have been studied by electronic calculations at a variety of levels of theory up to CBS-APNO. The results are in very good agreement with the best previous calculations. For

H<sub>2</sub>CNH<sup>2+</sup>, higher correlated methods, such as CCSD and BD, reveal that it is a saddle point rather than a shallow local minimum. The dissociations of neutral and charged H<sub>2</sub>CNH dissociation have been simulated by ab initio classical trajectories at the B3LYP/6-311G(d,p) level of theory. For the initial energies selected, many of the trajectories dissociate directly to produce H<sup>+</sup>, H atom, or H<sub>2</sub>. However, in a sizable fraction of the trajectories, there was substantial migration of the hydrogen within the molecule before dissociation occurred. Hydrogen atom was the preferred dissociation product for the neutral and the monocation. Elimination of H<sub>2</sub> was seen in 20% of the trajectories for the neutral and in 5% of the trajectories for the monocation. The dication and trication produced only H<sup>+</sup>. For the monocation and dication, HCNH<sup>+</sup> was formed in 85–90% of the dissociating trajectories.

**Acknowledgment.** This work was supported by a grant from the National Science Foundation. Computer time on Wayne State University computer grid is gratefully acknowledged.

**Supporting Information Available:** Geometries, relative energies, and SCF stabilities of structures on the CH<sub>2</sub>NH<sup>n+</sup> potential energy surface; relative energy and relaxed scans of H<sub>2</sub>CNH<sup>2+</sup> → H<sub>2</sub>NCH<sup>2+</sup> at various levels of theory; movies of the trajectories in Figure 5; and the complete ref 49. This material is available free of charge via the Internet at <http://pubs.acs.org>.

## References and Notes

- Pearson, R.; Lovas, F. J. *J. Chem. Phys.* **1977**, *66*, 4149–4156.
- Peel, J. B.; Willett, G. D. *J. Chem. Soc., Faraday Trans. 2* **1975**, *71*, 1799–1804.
- Hamada, Y.; Hashiguchi, K.; Tsuboi, M.; Koga, Y.; Kondo, S. *J. Mol. Spectrosc.* **1984**, *105*, 70–80.
- Bock, H.; Dammel, R. *Angew. Chem., Int. Ed. Engl.* **1987**, *26*, 504–526.
- Bock, H.; Dammel, R. *J. Am. Chem. Soc.* **1988**, *110*, 5261–5269.
- Dickens, J. E.; Irvine, W. M.; DeVries, C. H.; Ohishi, M. *Astrophys. J.* **1997**, *479*, 307–312.
- Milligan, D. E. *J. Chem. Phys.* **1961**, *35*, 1491–1497.
- Jacox, M. E.; Milligan, D. E. *J. Mol. Spectrosc.* **1975**, *56*, 333–336.
- Duxbury, G.; Kato, H. *Faraday Discuss.* **1981**, *71*, 97–110.
- Halonen, L.; Duxbury, G. *J. Chem. Phys.* **1985**, *83*, 2078–2090.
- Halonen, L.; Duxbury, G. *J. Chem. Phys.* **1985**, *83*, 2091–2096.
- Halonen, L.; Duxbury, G. *Chem. Phys. Lett.* **1985**, *118*, 246–251.
- Tešlja, A.; Nizamov, B.; Dagdigian, P. J. *J. Phys. Chem. A* **2004**, *108*, 4433–4439.
- Holmes, J. L.; Lossing, F. P.; Mayer, P. M. *Chem. Phys. Lett.* **1992**, *198*, 211–213.
- De Oliveira, G.; Martin, J. M. L.; Silwal, I. K. C.; Liebman, J. F. *J. Comput. Chem.* **2001**, *22*, 1297–1305.
- Pople, J. A.; Raghavachari, K.; Frisch, M. J.; Binkley, J. S.; Schleyer, P. v. R. *J. Am. Chem. Soc.* **1983**, *105*, 6389–6398.
- Nguyen, M. T.; Rademakers, J.; Martin, J. M. L. *Chem. Phys. Lett.* **1994**, *221*, 149–155.
- Nguyen, M. T.; Sengupta, D.; Ha, T. K. *J. Phys. Chem.* **1996**, *100*, 6499–6503.
- Sumathi, R. *J. Mol. Struct. (THEOCHEM)* **1996**, *364*, 97–106.
- Roithova, J.; Schroder, D.; Schwarz, H. *Eur. J. Org. Chem.* **2005**, 3304–3313.
- Demuyneck, J.; Fox, D. J.; Yamaguchi, Y.; Schaefer, H. F. *J. Am. Chem. Soc.* **1980**, *102*, 6204–6207.
- Gonzalez, C.; Schlegel, H. B. *J. Am. Chem. Soc.* **1992**, *114*, 9118–9122.
- Richards, C.; Meredith, C.; Kim, S. J.; Quelch, G. E.; Schaefer, H. F. *J. Chem. Phys.* **1994**, *100*, 481–489.
- Arenas, J. F.; Marcos, J. L.; Otero, J. C.; Sanchez-Galvez, A.; Soto, J. *J. Chem. Phys.* **1999**, *111*, 551–561.
- Kemnitz, C. R.; Ellison, G. B.; Karney, W. L.; Borden, W. T. *J. Am. Chem. Soc.* **2000**, *122*, 1098–1101.
- Polce, M. J.; Kim, Y. J.; Wesdemiotis, C. *Int. J. Mass Spectrom.* **1997**, *167*, 309–315.
- Larson, C.; Ji, Y. Y.; Samartzis, P.; Wodtke, A. M.; Lee, S. H.; Lin, J. J. M.; Chaudhuri, C.; Ching, T. T. *J. Chem. Phys.* **2006**, *125*, 133302.

- (28) Sumathi, R.; Nguyen, M. T. *J. Phys. Chem. A* **1998**, *102*, 8013–8020.
- (29) Tachikawa, H.; Iyama, T.; Fukuzumi, T. *Astron. Astrophys.* **2003**, *397*, 1–6.
- (30) Metropoulos, A.; Thompson, D. L. *J. Mol. Struct. (THEOCHEM)* **2007**, *822*, 125–132.
- (31) Burgers, P. C.; Holmes, J. L.; Terlouw, J. K. *J. Am. Chem. Soc.* **1984**, *106*, 2762–2764.
- (32) Flammang, R.; Nguyen, M. T.; Bouchoux, G.; Gerbaux, P. *Int. J. Mass Spectrom.* **2000**, *202*, A8–A26.
- (33) Curtis, R. A.; Farrar, J. M. *J. Chem. Phys.* **1986**, *84*, 127–134.
- (34) Frisch, M. J.; Raghavachari, K.; Pople, J. A.; Bouma, W. J.; Radom, L. *J. Chem. Phys.* **1983**, *75*, 323–329.
- (35) Uggerud, E.; Schwarz, H. *J. Am. Chem. Soc.* **1985**, *107*, 5046–5048.
- (36) Sana, M.; Leroy, G.; Hilali, M.; Nguyen, M. T.; Vanquickenborne, L. G. *J. Chem. Phys. Lett.* **1992**, *190*, 551–556.
- (37) Pearson, P. K.; Schaefer, H. F., III. *Astrophys. J.* **1974**, *192*, 33–36.
- (38) Conrad, M. P.; Schaefer, H. F., III. *Nature* **1978**, *274*, 456–457.
- (39) Allen, T. L.; Goddard, J. D.; Schaefer, H. F., III. *J. Chem. Phys.* **1980**, *73*, 3255–3263.
- (40) Defrees, D. J.; McLean, A. D. *J. Am. Chem. Soc.* **1985**, *107*, 4350–4351.
- (41) Defrees, D. J.; Binkley, J. S.; Frisch, M. J.; McLean, A. D. *J. Chem. Phys.* **1986**, *85*, 5194–5199.
- (42) Hansel, A.; Scheiring, C.; Glantschnig, M.; Lindinger, W.; Ferguson, E. E. *J. Chem. Phys.* **1998**, *109*, 1748–1750.
- (43) Peterson, K. A.; Mayrhofer, R. C.; Woods, R. C. *J. Chem. Phys.* **1990**, *93*, 4946–4953.
- (44) Koch, W.; Frenking, G.; Schwarz, H. *Naturwissenschaften* **1984**, *71*, 473–474.
- (45) Murrell, J. N.; Derzi, A. A. *J. Chem. Soc., Faraday Trans. 2* **1980**, *76*, 319–323.
- (46) von Niessen, W.; Cederbaum, L. S.; Domcke, W.; Dierksen, G. H. F. *Mol. Phys.* **1976**, *32*, 1057–1061.
- (47) Koch, W.; Heinrich, N.; Schwarz, H. *J. Am. Chem. Soc.* **1986**, *108*, 5400–5403.
- (48) Wong, M. W.; Yates, B. F.; Nobes, R. H.; Radom, L. *J. Am. Chem. Soc.* **1987**, *109*, 3181–3187.
- (49) Frisch, M. J.; *Gaussian Development Version*, Revision F.02; Gaussian, Inc.: Wallingford, CT, 2007.
- (50) Becke, A. D. *J. Chem. Phys.* **1993**, *98*, 1372–1377.
- (51) Becke, A. D. *J. Chem. Phys.* **1993**, *98*, 5648–5652.
- (52) Lee, C.; Yang, W.; Parr, R. D. *Phys. Rev. B* **1988**, *37*, 785–789.
- (53) Moller, C.; Plesset, M. S. *Phys. Rev.* **1934**, *46*, 618–622.
- (54) Pople, J. A.; Head-Gordon, M.; Raghavachari, K. *J. Chem. Phys.* **1987**, *87*, 5968–5975.
- (55) Seeger, R.; Pople, J. A. *J. Chem. Phys.* **1977**, *66*, 3045–3050.
- (56) Montgomery, J. A.; Ochterski, J. W.; Peterson, G. A. *J. Chem. Phys.* **1994**, *101*, 5900–5909.
- (57) Bakken, V.; Millam, J. M.; Schlegel, H. B. *J. Chem. Phys.* **1999**, *111*, 8773–8777.
- (58) Millam, J. M.; Bakken, V.; Chen, W.; Hase, W. L.; Schlegel, H. B. *J. Chem. Phys.* **1999**, *111*, 3800–3805.
- (59) Stoer, J.; Bulirsch, R. *Introduction to Numerical Analysis*; Springer-Verlag: New York, 1980.
- (60) Hase, W. L. In *Encyclopedia of Computational Chemistry*; Schleyer, P. v. R., Allinger, N. L., Clark, T., Gasteiger, J., Kollman, P. A., Schaefer, H. F., III, Schreiner, P. R., Eds.; Wiley: Chichester, U.K., 1998; p 402–407.
- (61) Peshlherbe, G. H.; Wang, H.; Hase, W. L. *Adv. Chem. Phys.* **1999**, *105*, 171–201.
- (62) Suits, A. G. *Acc. Chem. Res.* **2008**, *41*, 873–881.
- (63) Rubio-Lago, L.; Amaral, G. A.; Arregui, A.; Izquierdo, J. G.; Wang, F.; Zauris, D.; Kitsopoulos, T. N.; Banares, L. *Phys. Chem. Chem. Phys.* **2007**, *9*, 6123–6127.
- (64) Lahankar, S. A.; Chambreau, S. D.; Zhang, X. B.; Bowman, J. M.; Suits, A. G. *J. Chem. Phys.* **2007**, *126*, 044314.
- (65) Lahankar, S. A.; Chambreau, S. D.; Townsend, D.; Suits, F.; Farnum, J.; Zhang, X. B.; Bowman, J. M.; Suits, A. G. *J. Chem. Phys.* **2006**, *125*, 044303.
- (66) Houston, P. L.; Kable, S. H. *Proc. Natl. Acad. Sci.* **2006**, *103*, 16079–16082.
- (67) Chambreau, S. D.; Townsend, D.; Lahankar, S. A.; Lee, S. K.; Suits, A. G. *R. Swedish Acad. Sci.* **2006**, C89–C93.
- (68) Townsend, D.; Lahankar, S. A.; Lee, S. K.; Chambreau, S. D.; Suits, A. G.; Zhang, X.; Rheinecker, J.; Harding, L. B.; Bowman, J. M. *Science* **2004**, *306*, 1158–1161.
- (69) Bair, R. A.; Dunning, T. H. *J. Chem. Phys.* **1985**, *82*, 2280–2294.
- (70) ter Horst, M. A.; Schatz, G. C.; Harding, L. B. *J. Chem. Phys.* **1996**, *105*, 558–571.
- (71) Sharma, A. R.; Wu, J. Y.; Braams, B. J.; Carter, S.; Schneider, R.; Shepler, B.; Bowman, J. M. *J. Chem. Phys.* **2006**, *125*, 224306.
- (72) Psciuk, B. T.; Benderskii, V. A.; Schlegel, H. B. *Theor. Chem. Acc.* **2007**, *118*, 75–80.
- (73) Glukhovtsev, M. N.; Bach, R. D. *J. Chem. Phys. Lett.* **1998**, *286*, 51–55.
- (74) Lindh, R.; Rice, J. E.; Lee, T. J. *J. Chem. Phys.* **1991**, *94*, 8008–8014.
- (75) Liang, C.; Hamilton, T. P.; Schaefer, H. F., III. *J. Chem. Phys.* **1990**, *92*, 3653–3658.
- (76) Curtiss, L. A.; Pople, J. A. *J. Chem. Phys.* **1988**, *88*, 7405–7409.
- (77) Pople, J. A. *J. Chem. Phys. Lett.* **1987**, *137*, 10–12.
- (78) Lindh, R.; Roos, B. O.; Kraemer, W. P. *J. Chem. Phys. Lett.* **1987**, *139*, 407–416.
- (79) Lee, T. J.; Schaefer, H. F., III. *J. Chem. Phys.* **1986**, *85*, 3437–3443.
- (80) Gill, P. M. W.; Radom, L. *J. Am. Chem. Soc.* **1988**, *110*, 5311–5314.